

fRevolution — relativistic cosmological simulations in $f(R)$ gravity. Part I. Methodology

Lorenzo Reverberi^a and David Daverio^b

^aCEICO, Institute of Physics of the Czech Academy of Sciences,
Na Slovance 2, 18221 Praha 8, Czech Republic

^bCentre for Theoretical Cosmology,
Department of Applied Mathematics and Theoretical Physics,
Wilberforce Road, Cambridge CB3 0WA, United Kingdom

E-mail: lorenzo.reverberi@fzu.cz, dd415@cam.ac.uk

Received May 28, 2019

Revised June 22, 2019

Accepted June 27, 2019

Published July 22, 2019

Abstract. We present the new relativistic cosmological particle-mesh code `fRevolution`, based on `gevolution` [1], aimed at simulating non-linear structure formation in $f(R)$ gravity. We introduce the general framework and approximation scheme, and the system of equations used to solve for the full set of gravitational perturbations. We show results for a point mass field and for cosmological simulations in the Hu-Sawicki model, and compare them to those of existing Newtonian codes. A more detailed analysis and discussion of our solutions will be carried out in a following paper [2].

Keywords: cosmological simulations, modified gravity, power spectrum, cosmic web

ArXiv ePrint: [1905.07345](https://arxiv.org/abs/1905.07345)

Contents

1	Introduction	1
1.1	Metric	2
1.2	$f(R)$ gravity	2
2	Cosmological background	4
3	Perturbations	5
3.1	Scalaron field: trace equation	5
3.1.1	Relaxation solver	6
3.1.2	Change of variable	8
3.2	Gravitational potential: 00 equation	8
3.3	Vector field (elliptic constraint): $0i$ equation	9
3.4	Traceless ij equation	9
3.4.1	Spin-0 mode	10
3.4.2	Spin-1 mode	10
4	The Newtonian limit	10
5	Results	11
5.1	Point mass	12
5.2	Cosmological simulations	13
5.2.1	Matter power spectrum	13
5.2.2	Vector modes	14
5.2.3	Curvature	14
5.2.4	Gravitational slip	15
6	Conclusions	15

1 Introduction

The current and upcoming large scale structure surveys will be able to test cosmological structure formation with unprecedented precision. To properly understand and interpret this data, we therefore need to increase the precision of our theoretical prediction as well. The standard approach to investigate the non-linear process of structure formation is via N-body simulations [3–5], which however ignore any relativistic effect. Nevertheless, recent works have shown that it is possible to overcome this intrinsic limitation by interpreting the predictions of a Newtonian simulation in a relativistic context [6–11]. Such approach is well defined in the weak field approximation [7, 12], and allows to rely on Newtonian N-body codes to predict the matter dynamics of a relativistic theory such as General Relativity (GR). It is worth noting that it is possible to include relativistic effect in the initial conditions [13, 14], include relativistic species [15, 16] and, finally, to reconstruct relativistic observables [11].

On the other hand, in the Newtonian framework, the scale factor is completely decoupled from the evolution of matter and therefore needs to be set by hand. Therefore when one wants to implement dynamical dark energy or modified gravity theories, even if such theory

aims to modify the dynamic of the scale factor, the latter is *de facto* reconstructed and set by hand, or taken to be the one of the Λ -Cold Dark Matter concordance model (Λ CDM) [17–25]. While this is justified in first approximation for most viable alternative models, we cannot expect to be able to capture all the new dynamics following this approach, which thus might limit our ability to constrain these theories.

This motivates the creation of the code `gevolution`, based on GR and directly based on the weak field approximation [1, 26, 27]. In this paper, we propose a method to extend it to $f(R)$ gravity models and discuss its implementation in the new code `fRevolution` and the first results.

1.1 Metric

We consider the line element of a perturbed FLRW metric in the Poisson gauge

$$ds^2 = a^2(\tau) \left[-(1 + 2\Psi)d\tau^2 - 2B_i dx^i d\tau + (1 - 2\Phi)\delta_{ij} dx^i dx^j + h_{ij} dx^i dx^j \right], \quad (1.1)$$

where $a(\tau)$ is the cosmological scale factor, τ is the conformal time, and x^i are the comoving Cartesian coordinates. As usual, Greek indices run through all spacetime dimensions, while Latin indices run only on space-like dimensions. An overdot will denote derivative with respect to τ , a bar will denote background quantities and a tilde will denote Fourier transforms. The Hubble parameter is defined as $\mathcal{H} \equiv \dot{a}/a$.

The Poisson gauge corresponds to choosing B_i divergenceless, and h_{ij} traceless and divergenceless,¹ that is

$$\delta^{ij} \partial_i B_j = 0, \quad \delta^{ij} h_{ij} = \delta^{ij} \partial_i h_{jk} = 0. \quad (1.2)$$

We can maintain these even beyond the linear level provided that we remain in the weak field regime, where all the metric perturbations remain small $\ll 1$. Following the `gevolution` prescription, we also define the gravitational slip

$$\chi \equiv \Phi - \Psi, \quad (1.3)$$

and where convenient we will use the auxiliary field

$$\mathcal{B}_i \equiv a^{-2} B_i. \quad (1.4)$$

1.2 $f(R)$ gravity

Our goal is to study structure formation in $f(R)$ gravity. Among the possible modified gravity alternatives for cosmic acceleration [28–30], $f(R)$ gravity is one of the more popular and well-studied classes of theories. There is an extensive literature on $f(R)$ gravity and its cosmological implications, for a review see for instance [31–33] and references therein.

¹We should point out that in the present version of the code we neglect the tensor perturbations h_{ij} and their back-reaction on the particle evolution. Firstly, the effect of h_{ij} is much smaller than that of B_i which is itself much smaller than that of the standard scalar potentials Φ and Ψ . Secondly, resolving the full dynamics of massless tensor perturbations is computationally extremely expensive. One can still recover the approximate but typically accurate configuration of h_{ij} at each time by neglecting the time derivatives. See the original `gevolution` paper [1] for details on this point.

The action of the theory is²

$$S = \frac{1}{16\pi G} \int d^4x \sqrt{-g} F(R) \equiv \frac{1}{16\pi G} \int d^4x \sqrt{-g} [R + f(R)] + S_m[\psi; g_{\mu\nu}], \quad (1.5)$$

where f is a non-linear function of the Ricci scalar R . The field equations read

$$(1 + f_R)R_{\mu\nu} - \frac{R + f}{2} g_{\mu\nu} + \square_{\mu\nu} f_R = 8\pi G T_{\mu\nu}, \quad (1.6)$$

where we denoted $\square_{\mu\nu} \equiv g_{\mu\nu} \square - \nabla_\mu \nabla_\nu$ for compactness.

Among the $f(R)$ models relevant for the cosmic acceleration, the Hu-Sawicki model [34] is likely the most studied and tested at the level of cosmological background, linear perturbations, and Solar System (post-Newtonian approximation) [30, 35–39], and at the non-linear level with the use of simulations [17–19, 21]. These studies include possible degeneracies with other effects produced, for instance, by massive neutrinos [40]. The model is given by

$$f(R) = -m^2 \frac{c_1 (R/m^2)^n}{1 + c_2 (R/m^2)^n}, \quad (1.7)$$

where typically m^2 is of the order of the present curvature of the Universe. At large curvatures, this can be approximated by

$$f \approx -m^2 \frac{c_1}{c_2} + m^2 \frac{c_1}{c_2^2} \left(\frac{m^2}{R}\right)^n, \quad f_R \approx -\frac{n c_1}{c_2^2} \left(\frac{m^2}{R}\right)^{n+1} \quad (1.8)$$

Moreover, in the limit $c_1/c_2^2 \rightarrow 0$ at fixed c_1/c_2 the solutions are approximately [34]

$$R \approx 8\pi G \rho_m - 2f \approx 8\pi G \rho_m + 2m^2 \frac{c_1}{c_2}, \quad (1.9)$$

so choosing

$$\frac{c_1}{c_2} = \frac{16\pi G \rho_0 \Omega_\Lambda}{m^2} \quad (1.10)$$

will produce the observed accelerated background expansion. In most situations, the single parameter

$$f_{R_0} \equiv f_R(R_0) \approx -\frac{n c_1}{c_2^2} \left(\frac{m^2}{R_0}\right)^{n+1} \quad (1.11)$$

where $R_0 = 8\pi G \rho_0 (\Omega_m + 4\Omega_\Lambda)$ is the present cosmological curvature, is enough to essentially specify all the model dynamics, and it is generically found that for small enough values of $|f_{R_0}| \lesssim 10^{-5}$, the Hu-Sawicki model is in agreement with all existing observations.³ Operationally, specifying f_{R_0} , m^2 and n completely determines c_1 and c_2 once we impose the condition (1.10). In our simulations, we take $n = 1$ and consider three values of $|f_{R_0}| = 10^{-4}, 10^{-5}, 10^{-6}$ (see later for more details).

²We choose to work in the Jordan frame, where matter is minimally coupled to gravity so that the geodesics are the same as in GR. Alternatively, one can perform a conformal transformation to the Einstein frame, where the gravitational action is Einstein-Hilbert $S \sim \int d^4x \tilde{R}(\tilde{g}_{\mu\nu})$, but matter is coupled to a different metric than $\tilde{g}_{\mu\nu}$, so that the additional complexity resides in computing non-standard geodesics instead of non-standard evolution for the metric perturbations. Both approaches are equally valid and must lead to the same observable predictions.

³Possible issues related to the quasi-static approximation and to past singularities [41–45] suggest that we might be able to put even stronger constraints once these effects are taken into account; however, these issues are beyond the scope of this work and we will not consider them further.

2 Cosmological background

Because we work in the Jordan frame, the matter evolution of the different species remains the same as in GR, so that we only need the scale factor and the present (or initial) abundances in order to compute the background density and pressure:

$$\bar{\rho} = \bar{T}_0^0 = \sum_i \Omega_i a^{-3(1+w_i)} \quad \bar{P} \delta_k^j = \bar{T}_k^j = \delta_k^j \sum_i \Omega_i w_i a^{-3(1+w_i)} \quad (2.1)$$

where as usual

$$w_i = \begin{cases} 0 & \text{non relativistic matter: baryons, CDM} \\ 1/3 & \text{relativistic species, radiation} \\ -1 & \text{cosmological constant} \end{cases} \quad (2.2)$$

The background equations are given by

$$(1 + \bar{f}_R) \bar{R}_{\mu\nu} + \frac{\bar{R} + \bar{f}}{2} \bar{g}_{\mu\nu} + \bar{\square}_{\mu\nu} \bar{f}_R = 8\pi G \bar{T}_{\mu\nu}, \quad (2.3)$$

and their trace is

$$3\bar{f}_R^{\ddot{}} + 6\mathcal{H}\dot{\bar{f}}_R + (2\bar{f} + \bar{R} - \bar{f}_R \bar{R}) a^2 = -8\pi G a^2 \bar{T}_\mu^\mu, \quad (2.4)$$

which we can rewrite as

$$3\bar{f}_{RR} \bar{R}^{\ddot{}} + 3\bar{f}_{RRR} \bar{R}^{\dot{}}^2 + 6\mathcal{H}\bar{f}_{RR} \bar{R}^{\dot{}} + (2\bar{f} + \bar{R} - \bar{f}_R \bar{R}) a^2 = -8\pi G a^2 \bar{T}_\mu^\mu. \quad (2.5)$$

Although for $f(R)$ models of cosmic acceleration such as Hu-Sawicki the background is essentially that of Λ CDM at large curvatures, this is not necessarily true at very late times and surely not necessarily true for a generic $f(R)$ model. To facilitate extending our framework to other models and parameters, we decided to keep the background solver completely general. Moreover, because we are interested in looking for large scale relativistic effects, like back-reaction, we should make sure that the correct background is subtracted when calculating the perturbation equations lest we introduce unphysical homogeneous modes in the perturbations. Notice in particular that in general we will *not* have

$$\bar{R} = -8\pi G \bar{T}, \quad (2.6)$$

because of oscillatory solutions and/or of Λ -like components in the $f(R)$ solutions, which are not present explicitly in the matter energy-momentum tensor. In the code, we solve (2.5) using a Runge-Kutta-Fehlberg method [46] starting from the ‘‘GR’’ initial conditions

$$\begin{aligned} \mathcal{H}_{\text{in}} &= \frac{8\pi G}{3} (\Omega_m a_{\text{in}}^{-3} + \Omega_r a_{\text{in}}^{-4} + \Omega_\Lambda) \\ R_{\text{in}} &= 8\pi G (\Omega_m a_{\text{in}}^{-3} + 4\Omega_\Lambda) \\ \dot{R}_{\text{in}} &= -24\pi G \mathcal{H}_{\text{in}} \Omega_m a_{\text{in}}^{-3} \end{aligned} \quad (2.7)$$

deep in the matter-domination era, typically at redshift $z_{\text{in}} = (1 + a_{\text{in}})^{-1} \sim 100$.

In order to resolve the curvature and Hubble oscillations, one must choose a time step smaller than the typical oscillation time, which is roughly

$$\tau_{\text{osc}}^2 \simeq a \bar{f}_{RR}^{-1}. \quad (2.8)$$

3 Perturbations

In order to remove the background we expand each quantity Q as

$$Q = \bar{Q} + \delta Q, \quad (3.1)$$

keeping in mind that the background quantities of f and its derivatives are computed at $R = \bar{R}$. For convenience, we define the *scalon* field

$$\delta f_R \equiv \delta f_R = f_R - \bar{f}_R. \quad (3.2)$$

The perturbation equations then read

$$(1 + \bar{f}_R)\delta R_{\mu\nu} + \bar{R}_{\mu\nu}\delta f_R - \frac{\bar{R} + \bar{f}}{2}\delta g_{\mu\nu} - \frac{\delta R + \delta f}{2}(\bar{g}_{\mu\nu} + \delta g_{\mu\nu}) + (\delta\bar{\square}_{\mu\nu})f_R + \bar{\square}_{\mu\nu}\delta f_R = 8\pi G\delta T_{\mu\nu} \quad (3.3)$$

So far these are fully general, and do not assume small perturbations. Naturally, we do expect some perturbations to be indeed small, which simplifies the problem greatly.

Matter and curvature perturbations, that is $\delta T_0^0/\bar{T}_0^0$ and $\delta R/\bar{R}$, and particle velocities are kept at all orders, which allows us to study non-linear structure formation and relativistic or quasi-relativistic particle motion, such as CDM that has undergone rare extreme accelerations, and also intrinsically relativistic species like massive neutrinos.

Metric perturbations are assumed small and are normally kept at first order. However, we also keep terms quadratic in Φ provided that they contain two space derivatives (e.g. $\Phi\Delta\Phi$, etc.), which makes sense since the Poisson equation (not exact in GR nor $f(R)$), but qualitatively accurate nonetheless) dictates $\partial^2\Phi \propto \delta\rho$ and we are keeping $\delta\rho/\bar{\rho}$ at all orders.

We assume as usual that $f_R \ll 1$ as well as $\delta f_R \ll 1$, although the latter can be of the same order of magnitude and even larger than \bar{f}_R , and could be a “large” perturbation in the same sense as Φ . The scalaron appears in the equations in a way similar to that of Φ , contributing to the fifth-force effects of $f(R)$, and also directly sources the gravitational slip χ (see section 3.4.1), so we might risk losing potentially important features of the solutions by neglecting terms containing it.

Furthermore, we follow the standard approach and work in the quasi-static approximation, which consists in neglecting time derivatives. Therefore, we neglect $\delta\ddot{f}_R$, but unlike in other works which are based on the strictly Newtonian version of $f(R)$, we do keep the term proportional to $\mathcal{H}\delta\dot{f}_R$, as we do for Φ (see section 3.2). Our approximation scheme is summarised in table 1.

3.1 Scalon field: trace equation

We begin by considering the trace equation to update the scalaron field. Following the prescriptions in table 1, we obtain

$$(1 + 2\Phi)\Delta\delta f_R - 2\mathcal{H}\delta\dot{f}_R + \frac{a^2}{3}[f_R\delta R - 2\delta f + \bar{R}\delta f_R] = \frac{a^2}{3}(\delta R + 8\pi G\delta T). \quad (3.4)$$

Keep in mind that $\delta R = \delta R(f_R)$ and $\delta f = \delta f(f_R)$. This equation is a convenient choice as the first equation to solve in the code (after updating the energy-momentum tensor) because metric perturbations (and in fact only Φ) enter the equation only in a sub-leading term ($\Phi\Delta\delta f_R \ll \Delta\delta f_R$), so the error we make in using the old value of Φ will be negligible.

Quantity	Order
$\Phi, \dot{\Phi}, \ddot{\Phi}, \delta f_R, \delta \dot{f}_R, \chi, \dot{\chi}, \ddot{\chi}$	ϵ
$\Phi_{,i}, \dot{\Phi}_{,i}, \delta f_{R,i}, \delta \dot{f}_{R,i}, \chi_{,i}, \dot{\chi}_{,i}$	$\sqrt{\epsilon}$
$\Phi_{,ij}, \delta f_{R,ij}, \chi_{,ij}$	1
$B_i, \dot{B}_i, \ddot{B}_i, B_{i,j}, \dot{B}_{i,j}, \ddot{B}_{i,j}$	ϵ
$h_{ij}, \dot{h}_{ij}, \ddot{h}_{ij}, h_{ij,k}, \dot{h}_{ij,k}, h_{ij,k\ell}$	ϵ
$\delta T_0^0 / \bar{T}_0^0, \delta R / \bar{R}$	1
T_i^0 / \bar{T}_0^0	$\sqrt{\epsilon}$
Π_{ij} / \bar{T}_0^0	ϵ
v^i, q_i	1

Table 1. Orders of approximation used. The various fields are defined in section 1.1.

Note that the term containing $\delta \dot{f}_R$ is dealt with numerically by splitting it as

$$\delta \dot{f}_R = \delta f_R^{t-\frac{1}{2}} = \frac{\delta f_R^t - \delta f_R^{t-1}}{d\tau}. \quad (3.5)$$

The index t , though it has an obvious correspondence with the cosmological time, is simply a discrete index labelling the simulation steps.

3.1.1 Relaxation solver

The difficulty in solving (3.4) comes from the fact that the relation between δf_R and δR is in general (highly) non-linear so we cannot use standard spectral methods (e.g. FFT), rather we have to rely on relaxation methods. Schematically, we start from an equation of the form

$$U[\delta f_R] = S(T_{\mu\nu}, \delta f_R) \quad \Rightarrow \quad Y[\delta f_R, T_{\mu\nu}] \equiv U - S = 0. \quad (3.6)$$

In (3.6), U is a non-linear differential operator acting on δf_R , and the source term S can in principle contain terms depending on δf_R as well. Starting from an initial guess $\delta f_R = \delta f_R^{(0)}$, associated with a residual $r^{(0)}$

$$r^{(0)} \equiv Y[\delta f_R^{(0)}], \quad (3.7)$$

we implement a *Newton-Raphson* iterative method, defined by

$$\delta f_R^{(n+1)} = \delta f_R^{(n)} + \varepsilon^{(n)} \equiv \delta f_R^{(n)} - \frac{Y}{\partial Y / \partial (\delta f_R)} \Big|_{\delta f_R = \delta f_R^{(n)}}, \quad (3.8)$$

where the error $\varepsilon^{(n)}$ quantifies the correction between values of δf_R at consecutive iterations. Convergence is reached comparing the residual of the equation with some (small) pre-determined constant r_c :

$$\|Y^{(n)}\| < r_c, \quad (3.9)$$

where typically $\|\cdot\|$ denotes L_2 norm taken over the whole grid:

$$\|Y^{(n)}\|^2 = \sum_{i,j,k} (Y_{i,j,k}^{(n)})^2. \quad (3.10)$$

Notice that the index n denotes a progression in the relaxation, not in cosmological time. To clarify, eq. (3.8) defines a sequence which progressively approaches the solution of (3.6) at each time step. In this sense, an additional (fixed) index t is implied in each quantity in (3.8).

There are many possible sweeping strategies, the most popular and one of the easier to parallelise being the *red-black* scheme, in which one solves the equation for cells of the same colour as in the colours of a chess board (straightforwardly generalised to 3 spatial dimensions), and then solves for the remaining half. The reason why this scheme is particularly useful for parallelisation is that when discretised on a lattice labelled by the indices i, j, k and having cell size ℓ , eq. (3.4) only depends on the local value of δf_R and of its Laplacian, which is computed from the nearest neighbours:

$$\Delta \delta f_R^{i,j,k} = \frac{\delta f_R^{i+1,j,k} + \delta f_R^{i-1,j,k} + \delta f_R^{i,j+1,k} + \delta f_R^{i,j-1,k} + \delta f_R^{i,j,k+1} + \delta f_R^{i,j,k-1} - \delta f_R^{i,j,k}}{6\ell^2}. \quad (3.11)$$

Because the nearest neighbours of a black cell are red and vice versa, we can parallelise the update of all cells of one colour and afterwards update the remaining half.

Despite parallelising the relaxation, convergence often becomes increasingly slower as one approaches the exact solution. Formally, the issue is that the modes in the residual that have wavelengths longer than the grid size decrease more slowly than those with wavelengths comparable with the grid size. Therefore, especially for large grids, one often relies on multi-grid methods to speed up the convergence. Multi-grid algorithms speed up the convergence of these long wavelength modes by solving the equation on coarser grids (larger grid size), whose small-scale modes (in units of the grid size) correspond to larger scale modes in the finer grids.

For simplicity, we briefly illustrate the algorithm for two grids, but it can be easily generalised (see e.g. [47] for additional details). After a number of relaxation steps on the finer grid ℓ , which produce a guess δf_R^ℓ with residual

$$r^\ell = Y^\ell[\delta f_R^\ell], \quad (3.12)$$

we move to the coarser grid having cell size L (typically $L = 2\ell$) using the *restriction* operator⁴ $\mathcal{R}_{\ell \rightarrow L}$ on the scalaron and on the residual:

$$\delta f_{R,\text{old}}^L = \mathcal{R}_{\ell \rightarrow L}(\delta f_{R,\text{old}}^\ell), \quad r_{\text{old}}^L = \mathcal{R}_{\ell \rightarrow L}(r_{\text{old}}^\ell). \quad (3.13)$$

On the new grid, we perform additional relaxations steps solving the modified equation

$$Y^L[\delta f_{R,\text{new}}^L] = Y^L[\delta f_{R,\text{old}}^L] - r_{\text{old}}^L. \quad (3.14)$$

We then *prolong* the error $\varepsilon^L \equiv \delta f_{R,\text{new}}^L - \delta f_{R,\text{old}}^L$ from the coarser grid to the finer grid, and thus correct the guess for δf_R on the latter:

$$\delta f_{R,\text{new}}^\ell = \delta f_{R,\text{old}}^\ell + \mathcal{P}_{L \rightarrow \ell}(\varepsilon^L). \quad (3.15)$$

Additional relaxation steps are then performed on the finer grid, and if required the multigrid cycle can be repeated until the desired precision is achieved.

⁴The restriction/injection/fine-to-coarse and the prolongation/interpolation/coarse-to-fine operators define the mapping between fields on two grids with different cell sizes. We choose a tri-linear interpolation for the prolongation operator, and its adjoint or inverse (full-weighting) for the restriction. See e.g. [47] for details.

3.1.2 Change of variable

Depending on the specific $f(R)$ model, δf_R might only have a finite range of “healthy” values,⁵ and it may happen that the sequence (3.8) accidentally pushes δf_R outside this range. For instance, in the Hu-Sawicki model [34], the relation $R(f_R)$ is well-defined only for a definite sign of f_R , so clearly only a finite range of values of $\delta f_R \equiv f_R - \bar{f}_R$ is allowed. Where needed, as suggested in [17], we circumvent this problem by using the auxiliary variable u , defined as

$$f_R \equiv \bar{f}_R e^u \quad \Leftrightarrow \quad \delta f_R = \bar{f}_R (e^u - 1). \quad (3.16)$$

This is of course not the only possible choice, and in principle each model should be considered individually. Once we have a relation $R(u)$ that is well-defined on the whole real axis, we can convert $\delta f_R \rightarrow u$ on each lattice point, re-formulate the trace equation in terms of u , and apply a strategy analogous to (3.8), before converting back $u \rightarrow \delta f_R$. For the specific case (3.16), we have for example

$$\delta f_R^{(n)} + \varepsilon^{(n)} = \bar{f}_R \left(e^{u^{(n)} + \delta u^{(n)}} - 1 \right), \quad (3.17)$$

so expanding the right-hand side at first order in δu (we drop the subscript (n) for simplicity) we obtain

$$\begin{aligned} \delta f_R + r &\simeq \bar{f}_R (e^u + e^u \delta u - 1) = \delta f_R + \bar{f}_R e^u \delta u \\ &= \delta f_R + f_R \delta u \quad \Rightarrow \quad \delta u \simeq \frac{\varepsilon}{f_R}. \end{aligned} \quad (3.18)$$

In practice, we can skip converting between δf_R and u using the following sequence

$$\delta f_R^{(n+1)} = \bar{f}_R \left[\exp \left(u^{(n+1)} \right) - 1 \right] \simeq f_R^{(n)} \exp \left(\frac{\varepsilon^{(n)}}{f_R^{(n)}} \right) - \bar{f}_R, \quad (3.19)$$

where for clarity we remind the reader that $\varepsilon^{(n)}$ is given by (3.8).

3.2 Gravitational potential: 00 equation

Having solved the trace equation, we use the 00 equation to solve for Φ , putting all terms containing the scalaron in the source term:

$$\begin{aligned} \left(\Delta - \frac{3\mathcal{H}}{d\tau} - 3\mathcal{H}^2 \right) \Phi_t &= -4\pi G a^2 (1 - 4\Phi - f_R) \delta T_0^0 + \frac{1 - 2\Phi - f_R}{2} \Delta \delta f_R - \\ &\quad - \frac{3}{2} \mathcal{H}^2 (2\chi + \delta f_R) - \frac{1}{2} \delta^{ij} \Phi_{,i} (3\Phi + \delta f_R)_{,j} + \\ &\quad + \frac{R \delta f_R + \bar{f}_R \delta R - \delta f}{4} a^2 - \frac{3\mathcal{H}}{d\tau} \Phi - \frac{3\mathcal{H}}{2} \delta f_R \\ &\equiv S_0^0, \end{aligned} \quad (3.20)$$

where it is implied that $\Phi = \Phi_{t-1}$ and $\chi = \chi_{t-1}$ in the right-hand side. With this new source term, Φ_t is readily computed via

$$\tilde{\Phi}_t = - \left(k^2 + \frac{3\mathcal{H}}{d\tau} + 3\mathcal{H}^2 \right)^{-1} \tilde{S}_0^0, \quad (3.21)$$

which allows us to update both Φ_t and $\dot{\Phi}_{t-\frac{1}{2}}$ analogously to (3.5).

⁵This is not a generic feature of $f(R)$ models, but it occurs in several models designed to produce cosmic acceleration, including the Hu-Sawicki model. Typically, this happens whenever $f(R)$ and/or the relation $R \leftrightarrow f_R$ are ill-defined for $R < 0$, or when the unbounded interval $-\infty < R < \infty$ is mapped into a bounded interval for f_R .

3.3 Vector field (elliptic constraint): $0i$ equation

The $0i$ equation

$$\begin{aligned}
 -\frac{1}{2}\Delta B_i - B_i\Delta\Phi + \delta^{jk}B_j(\delta f_R - \Phi)_{,ik} - \mathcal{H}(2\Phi - 2\chi + \delta f_R)_{,i} - \\
 - 2\dot{\Phi}_{,i} + \delta\dot{f}_{R,i} - \dot{f}_R\Phi_{,i} - 2(\Phi - \chi)\delta\dot{f}_{R,i} = 8\pi G a^2 T_i^0,
 \end{aligned} \tag{3.22}$$

can be used to evolve the vector mode B_i via an elliptic constraint equation. Projecting (3.22) on the spin-1 component, using the operator

$$P_{(1)}^{ij} \equiv k^2\delta^{ij} - k^i k^j, \tag{3.23}$$

we obtain

$$\delta^{ij}(\widetilde{B}_i)_t = 2k^{-4}(k^2\delta^{ij} - k^i k^j) \text{ Fourier} \left\{ 8\pi G a^2 T_i^0 + B_i\Delta\Phi + \delta^{k\ell}B_k(\Phi - \delta f_R)_{,i\ell} \right\}. \tag{3.24}$$

3.4 Traceless ij equation

We finally consider the traceless part of the ij equations, namely

$$\begin{aligned}
 \left(\delta_k^i \delta_\ell^j - \frac{1}{3} \delta_{k\ell} \delta^{ij} \right) \left[\dot{B}_{(i,j)} + 2\mathcal{H}B_{(i,j)} + 2\Phi_{,i}(\Phi - \delta f_R)_{,j)} + \right. \\
 \left. + 2(2\Phi - \chi)\Phi_{,ij} - (1 + 2\Phi)\delta f_{R,ij} + \chi_{,ij} \right] = 8\pi G a^2 \Pi_{k\ell},
 \end{aligned} \tag{3.25}$$

where

$$\Pi_{ij} \equiv \left(\delta_{ik} \delta_j^\ell - \frac{1}{3} \delta_k^\ell \delta_{ij} \right) T_\ell^k, \tag{3.26}$$

and round brackets in indices denote symmetrisation:

$$A_{(i}B_{j)} \equiv \frac{A_i B_j + A_j B_i}{2}. \tag{3.27}$$

This equation will be used to evolve the gravitational slip χ (via its spin-0 projection), and possibly B_i (via the spin-1 projection) through a parabolic equation.

As mentioned previously, we are neglecting the tensor perturbations h_{ij} . They would enter these equations through a term proportional to $\dot{h}_{ij} + 2\mathcal{H}\dot{h}_{ij} - \Delta h_{ij}$, unchanged from GR to $f(R)$, inside the square brackets.

We move all non-linear terms and terms containing Φ and δf_R (already updated at this point of the cycle) to the right-hand side and project on the traceless part, obtaining

$$\begin{aligned}
 \dot{B}_{(i,j)} + 2\mathcal{H}B_{(i,j)} + \chi_{,ij} - \frac{1}{3}\delta_{ij}\Delta\chi = \\
 = 8\pi G a^2 \Pi_{ij} - \left(\delta_i^k \delta_j^\ell - \frac{1}{3} \delta^{k\ell} \delta_{ij} \right) [2\Phi_{,k}\Phi_{,\ell} + 2(2\Phi - \chi)\Phi_{,k\ell} - \delta f_{R,k\ell}] \\
 \equiv S_{ij} - \frac{1}{3}\delta_{ij}S + \delta f_{R,ij} - \frac{1}{3}\delta_{ij}\Delta\delta f_R.
 \end{aligned} \tag{3.28}$$

We kept δf_R separated from the rest of the source term in the right-hand side for reasons that will be clear shortly. Note also that

$$\dot{B}_i \equiv \partial_\tau(a^2 B_i) = a^2(\dot{B}_i + 2\mathcal{H}B_i), \tag{3.29}$$

so this is going to be the combination that is actually used to solve this equation. In Fourier space, we obtain

$$i a^{-2} \tilde{B}_{(i} k_{j)} - k_i k_j \tilde{\chi} + \frac{k^2}{3} \delta_{ij} \tilde{\chi} = \tilde{S}_{ij} - \frac{1}{3} \delta_{ij} \tilde{S} - k_i k_j \delta \tilde{f}_R + \frac{k^2}{3} \delta_{ij} \delta \tilde{f}_R. \tag{3.30}$$

3.4.1 Spin-0 mode

We first calculate χ by projecting on the spin-0 part, using the projection operator

$$P_{(0)}^{ij} \equiv k^2 \delta^{ij} - 3k^i k^j, \quad (3.31)$$

which yields

$$2k^4 \chi^t = (k^2 \delta^{ij} - 3k^i k^j) \tilde{S}_{ij}(\Phi^t, \chi^{t-1}) + 2k^4 \delta f_R^t, \quad (3.32)$$

so we finally obtain

$$\chi^t = \delta f_R^t + \text{Fourier}^{-1} \left\{ \frac{1}{2k^4} (k^2 \delta^{ij} - 3k^i k^j) \tilde{S}_{ij}(\Phi^t, \chi^{t-1}) \right\}. \quad (3.33)$$

Notably, we can avoid the computation of the scalaron-dependent terms in the source, and simply add δf_R to the final result, which is why we chose to keep those terms explicit in (3.28).

Eq. (3.33) is essentially showing how the new scalar is a source of anisotropic stress in $f(R)$ gravity theories. In fact, if one assumes that Φ and $T_{\mu\nu}$ are essentially the same as in GR,⁶ then it is the *difference* ($\chi - \delta f_R$) that is roughly equal to χ_{GR} (see also section 4), or equivalently

$$\chi_{f(R)} \approx \chi_{\text{GR}} + \delta f_R. \quad (3.34)$$

3.4.2 Spin-1 mode

Projecting on the spin-1 component, using the projector (3.23) through the contraction

$$P_{(1)}^{i\ell} k^j (\text{Equation})_{ij}, \quad (3.35)$$

where $P_{(1)}$ was defined in (3.23), finally yields, using the gauge condition $\tilde{\mathcal{B}}_i k^i = 0$,

$$\dot{\tilde{\mathcal{B}}}_i = -\frac{2ia^2}{k^4} \delta_{i\ell} (k^2 \delta^{j\ell} - k^j k^\ell) k^m \tilde{S}_{jm}. \quad (3.36)$$

The field $\tilde{\mathcal{B}}_i$ is then updated with a simple Euler criterion

$$\tilde{\mathcal{B}}_i^t = \tilde{\mathcal{B}}_i^{t-1} - \frac{2ia^2 d\tau}{k^4} \delta_{i\ell} (k^2 \delta^{j\ell} - k^j k^\ell) k^m \tilde{S}_{jm}. \quad (3.37)$$

4 The Newtonian limit

In order to make the comparison to existing codes more straightforward, in this section we present the Newtonian limit of our perturbation equations, and discuss the further assumptions typically made in a Newtonian framework. The Newtonian limit of (3.20) is essentially the $f(R)$ equivalent of the Poisson equation, which is

$$\Delta \Phi_N = 4\pi G a^2 \delta \rho, \quad (4.1)$$

where Φ_N is the Newtonian potential. Furthermore, the geodesic motion of non-relativistic test particles can be approximated by

$$\ddot{\mathbf{x}} = \ddot{\mathbf{x}}_{\text{GR}} \equiv -\nabla \Phi_{\text{GR}}. \quad (4.2)$$

⁶This is obviously not a good quantitative approximation, but it helps in understanding the qualitative effect of modified gravity on χ .

Several fundamental assumptions are being made in the Newtonian limit, namely that Φ_N is small so that the first order terms suffice, and that we are in the deep sub-horizon, quasi-static regime so that

$$\partial_t, \mathcal{H} \ll k. \quad (4.3)$$

We should also assume that $\delta P \ll \delta\rho$, as is the case if velocities are non-relativistic. Moreover, we are assuming that only the leading corrections to GR are relevant, which allows us to get rid of plenty of terms such as $f_R \ll 1$, $f_{RR}R \ll 1$ and so on. With these approximations, we find that the leading contribution to (3.20) is given by

$$\Delta\Phi = 4\pi G a^2 \delta\rho + \frac{1}{2}\Delta\delta f_R, \quad (4.4)$$

so that the correction to the field Φ , assuming that $\delta\rho$ evolves practically as in GR, is roughly

$$\Phi_{f(R)} \approx \Phi_{\text{GR}} + \frac{1}{2}\delta f_R. \quad (4.5)$$

Moreover, as we have seen in section 3.4.1, the gravitational slip χ (which vanishes identically in Newtonian gravity) is now sourced directly by the scalaron, so that

$$\chi \approx \chi_{\text{GR}} + \delta f_R. \quad (4.6)$$

These equations provide us with one the more intuitive ways to see how the additional scalar sources the gravitational potential and contributes as a fifth force, in fact the acceleration of a test particle will be

$$\ddot{\mathbf{x}} \simeq -\nabla\Psi = -\nabla(\Phi - \chi) \approx -\nabla\Phi_{\text{GR}} + \frac{1}{2}\nabla\delta f_R = \ddot{\mathbf{x}}_{\text{GR}} + \delta\ddot{\mathbf{x}}_{f(R)}. \quad (4.7)$$

Similarly, the Newtonian limit of the trace equation (3.4) reads

$$\Delta\delta f_R = \frac{a^2}{3}(\delta R - 8\pi G\delta\rho), \quad (4.8)$$

which in combination with the previous results yields

$$\Delta\Phi = a^2 \left(\frac{8\pi G}{3}\delta\rho + \frac{\delta R}{6} \right), \quad \Delta\Psi = a^2 \left(\frac{16\pi G}{3}\delta\rho - \frac{\delta R}{6} \right), \quad (4.9)$$

which are precisely the equations used in the pioneering [17].

In the Newtonian approximation, we replace (3.4) and (3.20) with (4.8) and (4.4), respectively. When computing the particle dynamics, we moreover neglect B_i and χ , as well as the standard relativistic corrections (typically of order $v^2/c^2 \ll 1$). See the original `gevolution` paper [1] for details.

5 Results

In this section we will present some results from our simulations and their comparison with Λ CDM and existing modified gravity codes [21, 22]. A more detailed discussion will appear in a following paper [2].

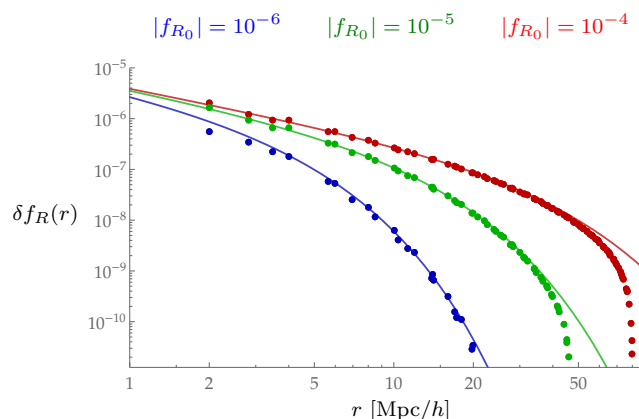


Figure 1. Point-mass solutions and comparison with the analytical prediction (5.3). Deviations at large radii are due to our periodic conditions whereas (5.3) assumes asymptotically flat boundary conditions.

5.1 Point mass

As a first test, we consider the static field produced by a point mass located in the centre of a $(256\text{Mpc}/h)^3$ cubic box (with periodic boundary conditions), solving on 128^3 grid points (hence the spatial resolution is $\ell_{\text{cell}} = 2\text{Mpc}/h$), and compare these results with the analytical solutions obtained linearising (4.8):

$$\Delta\delta f_R = \frac{\delta f_R}{3\bar{f}_{RR}} - \frac{8\pi G}{3}\delta\rho, \quad (5.1)$$

with a density field

$$\delta\rho = \begin{cases} 10^{-4}(N^3 - 1)\bar{\rho} & \text{point mass cell} \\ -10^{-4}\bar{\rho} & \text{elsewhere} \end{cases} \quad (5.2)$$

The formal solution for an actual point mass $\rho = m\delta^{(3)}(\mathbf{r})$ in an asymptotically flat Universe is trivially a Yukawa-like profile

$$\delta f_R = \frac{2Gm}{3} \frac{e^{-r/\sigma}}{r}, \quad (5.3)$$

where

$$\sigma^2 = 3\bar{f}_{RR}. \quad (5.4)$$

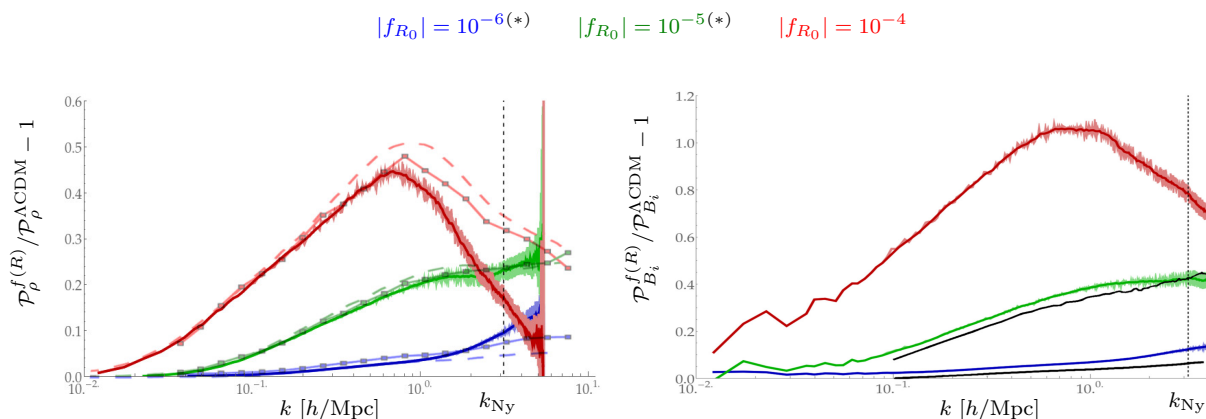
The conversion between m and (5.2) is given by

$$m \rightarrow 10^{-4}(N^3 - 1)\bar{\rho}V_{\text{cell}}, \quad (5.5)$$

where $V_{\text{cell}} = \ell_{\text{cell}}^3$ is the volume of a lattice cell. For $|f_{R_0}| = 10^{-6}$, we replace the point mass with a Gaussian profile

$$\rho \propto \exp\left(-\frac{r^2}{\ell_{\text{cell}}^2}\right), \quad (5.6)$$

because $\delta f_R > |f_{R_0}|$ at small distances, and hence the linear approximation fails. In all cases, we expect solutions to deviate from the analytical result nearest to the overdensity and to the boundaries of the box, due to finite resolution and finite size effects, respectively. Results are shown in figure 1.



(a) Results for the relative enhancement of the matter power spectrum compared to Λ CDM, compared to the results of [21] (dashed lines) and [22] (dots). The discrepancy for $|f_{R_0}| = 10^{-4}$ near the Nyquist scale k_{Ny} (dashed vertical line) most likely have no physical origin and are instead artifacts of unavoidable smoothing and finite resolution effects. Overall, our results and [21, 22] agree extremely well for $k \lesssim 0.25 k_{\text{Ny}}$ even when small scale differences are largest.

(b) Power excess for the vector modes B_i . Deviations are generically larger than those of $\delta\rho$ and follow a similar qualitative behaviour. As was remarked in the text, any departure from Λ CDM is not due to additional sources in the evolution equation for the vector modes, but to the indirect effect of changes in the scalar potentials and in the matter source. (*) For a direct comparison with the results of [49] (black solid lines), we used a slightly different cosmology than the other simulations and $|f_{R_0}| = 1.289 \times 10^{-5}, 1.289 \times 10^{-6}$.

Figure 2. Results for $\delta\rho$ and B_i .

5.2 Cosmological simulations

We performed three simulations of a $(512 \text{ Mpc}/h)^3$ comoving box with 512^3 grid points and the same number of CDM particles, for different values of $|f_{R_0}| = 10^{-4}, 10^{-5}, 10^{-6}$. This allows us to study the limit in which the model reduces essentially to Λ CDM and when instead deviations become significant. The other cosmological parameters used in the simulations are [48]: $h = 0.6736$, $\Omega_b h^2 = 0.02237$, $\Omega_c h^2 = 0.1200$, $n_s = 0.9649$, $A_s = 2.099 \times 10^{-9}$ (at 0.05 Mpc^{-1}). We should stress that these cosmological parameters are not the most up-to-date values available (see e.g. [48]) but were chosen for a direct comparison with the existing codes [21, 22]. We plan on using more recent values in an upcoming publication [2] in which we discuss our results in more detail.

5.2.1 Matter power spectrum

We present our results for the matter power spectrum in figure 2a, where we overlay our power spectra to those of MG-gadget [22]. We observe excellent agreement with [22] at all scales except for $|f_{R_0}| = 10^{-4}$ (where deviations from GR are most significant), where our solutions have a faster drop in the power excess around $k \gtrsim 1h/\text{Mpc}$. This is most likely due to the proximity to the Nyquist scale k_{Ny} , and in general we do not expect our results to be accurate and competitive with those of MG-gadget so close to k_{Ny} .⁷

⁷Notice that the results of the original `gevolution` code also deviate from those of Gadget at small scales $k \simeq k_{\text{Ny}}$, and that in particular *less* power is produced around those scales (see [1] for details).

Altogether, we can still state that our results for $|f_{R_0}| = 10^{-4}$ agree with those of existing codes very well, even in the non-linear regime, at scales larger than about a factor of 4–5 times the Nyquist scale; the agreement is even better and essentially perfect at any scale $k < k_{\text{Ny}}$ for $|f_{R_0}| = 10^{-5}, 10^{-6}$. Considering the intrinsic limitations of a fixed-grid approach compared to an adaptive mesh, we can consider this agreement very satisfactory.

5.2.2 Vector modes

In figure 2b we present our results for the power spectrum of vector modes B_i . We also compare our results with those of [49], in which vector modes are computed in a Post-Friedmannian framework. For this reason, we used slightly different cosmological parameters (see [49]) and the values $|f_{R_0}| = 10^{-4}, 1.289 \times 10^{-5}$ and 1.289×10^{-6} .

We can see that the power excess compared to Λ CDM is larger by roughly 100%, 30% and a few percent for $|f_{R_0}| = 10^{-4}, 10^{-5}$ and 10^{-6} respectively, at $k \simeq 1h/\text{Mpc}$. We should stress again that this excess is not due to any additional term appearing directly in the evolution equation for B_i , but indirectly due to how the scalar potentials (and its gradient, which sources the vector modes) and the matter source are modified because of the $f(R)$ contributions. It is therefore remarkable that the power excess is even larger than for Φ which is sourced by δf_R directly. The agreement with [49] is overall rather good but we do detect a slight excess of extra power. We plan to investigate this point further in a following publication.

5.2.3 Curvature

Next we present the solutions for the scalar curvature perturbations δR , in figure 3a. The figure shows the ratio of power spectra instead of the relative power excess as in the previous cases, because the differences from the Λ CDM solution

$$\delta R = -8\pi G \delta T \quad (5.7)$$

can be of several orders of magnitude and not at most of order unity as in the cases of matter and vector perturbations.

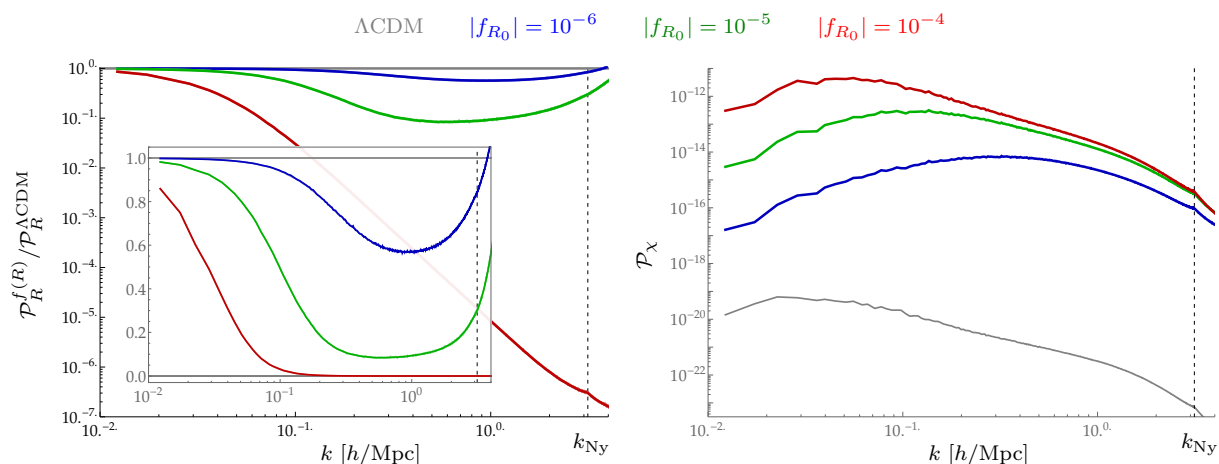
We see that the Λ CDM limit appears to be recovered in the appropriate limit as $|f_{R_0}|$ decreases, but we also notice that deviations are significant, especially at smaller scales, already at relatively small values of $|f_{R_0}|$ and rather strikingly for $|f_{R_0}| = 10^{-4}$ at basically all scales. While deviations in δR are not easily testable alone, as the main cosmological observable is the matter power spectrum, these results suggest that even in those cases in which deviations in $\delta\rho$ and Φ are relatively small, the linear expansion around some reference curvature⁸ \tilde{R} might give extremely inaccurate approximations to the real solution. For example, we can not assume

$$f_R(\tilde{R} + \delta R) \simeq \tilde{f}_R + \tilde{f}_{RR} \delta R \quad (5.8)$$

if $|\delta R/\tilde{R}| \sim 1$, and similarly for other derivatives. Moreover, this is typically exacerbated by the high non-linearity of the relation between f_R and R in $f(R)$ models relevant for cosmic acceleration

The conclusion is that one should be very careful when producing estimates for the effects of modified gravity in the approximation $R \simeq R^{\Lambda\text{CDM}}$, because this could be violated by many orders of magnitude even in those cases for which the gravitational potential and the matter power spectrum are not too different that in GR.

⁸Note that \tilde{R} needs not be the cosmological background curvature \bar{R} , but can be any “sensible” choice, for instance the GR solution $\tilde{R} = -8\pi GT$.



(a) Power spectra for the scalar curvature and comparison with the GR solution $\delta R = -8\pi G\delta T$. Although this solution is recovered in the appropriate limit, deviations are very significant even at relatively low $|f_{R0}|$ (see the text for a discussion on this point). The two plots show the same results in logarithmic and linear scale on the vertical axis.

(b) Power spectra of χ , compared with ΛCDM (grey line). As we can see, deviations can be enormous and remain large even at large scales and even for $|f_{R0}| = 10^{-6}$, for which value the other quantities of interest essentially recover the ΛCDM solutions.

Figure 3. Results for δR and χ .

5.2.4 Gravitational slip

We present our results for χ in figure 3b. In this case we show the actual power spectra instead of the relative power enhancement. As we have seen in section 3.4.1, the scalaron directly sources χ and so when δf_R is much larger than χ would be in GR, it completely dominates and we have essentially $\chi \approx \delta f_R$. Because δf_R can in principle be of the same order of magnitude as $|f_{R0}|$ and even larger, we can easily see how χ can be many orders of magnitude larger than in ΛCDM .

Interestingly, this is the only quantity for which in the case $|f_{R0}| = 10^{-6}$ we do not recover ΛCDM plus very small corrections, but instead deviations remain large, of several orders of magnitude, even at large scales. The possibility of detecting signatures of modified gravity using the gravitational slip is an interesting topic (see e.g. the recent [50]), and we plan on discussing some of these possibilities in an upcoming work [2].

6 Conclusions

We have presented the framework and first results from the code `fRevolution`, based on the relativistic code `gevolution` [1]. We have discussed the approximation scheme which only relies on the weak field limit of GR with no further assumption on the smallness of density and scalar curvature perturbations, nor on the smallness of the scalaron δf_R compared to \bar{f}_R . Moreover, we go beyond the Newtonian limit (see section 4) and take into account the Hubble friction when solving for the scalaron dynamics.

Overall, our results agree very well with analytical predictions in the case of the field produced by a point mass, and with existing (Newtonian) modified gravity codes for the

matter power spectrum. To our knowledge, we present for the first time direct results for the scalar curvature perturbations, which however can be computed even in a strictly Newtonian framework, and for the gravitational slip χ and frame dragging B_i which instead are intrinsically relativistic effects and can be computed in Newtonian codes only a posteriori under the assumption that Newtonian and relativistic solutions for Φ and δf_R are essentially the same.

For the chosen parameter values, we detect a power excess for vector modes of about a factor 2, and differences of several orders of magnitude for χ and δR compared to the Λ CDM predictions. While the impact of modified structure formation on the gravitational slip might provide interesting new directions to test and constrain modified gravity, the observed deviations from GR in the solutions for δR suggest that extra care should be taken, when formulating predictions in modified gravity based on the assumption that deviations from the GR curvature are small, namely that not only $|f_R| \ll 1$, but also that $|\delta R + 8\pi G\delta T| \ll |8\pi G\delta T|$. We plan to carry out a more extensive discussion and analysis of our results in an upcoming publication [2].

Acknowledgments

The authors would like to thank J. Adamek, M. Kunz and I. Sawicki for useful comments and discussions during the development and testing of the code, and Á. de la Cruz-Dombriz and P. Dunsby for their support and contribution during the early phases of the project. LR would like to thank the DAMTP, University of Cambridge for its hospitality. Early tests of the code have been carried out on the clusters *Zeus* at the University of Cape Town and *Baobab* at the University of Geneva. The final simulations have been carried out on *Koios* at the Institute of Physics of the Czech Academy of Sciences in Prague. DD is supported by an Advanced Postdoc.Mobility grant of the Swiss National Science Foundation. LR is supported by ESIF and MEYS (Project CoGraDS-CZ.02.1.01/0.0/0.0/15_003/0000437).

References

- [1] J. Adamek, D. Daverio, R. Durrer and M. Kunz, *gevolution: a cosmological N-body code based on General Relativity*, *JCAP* **07** (2016) 053 [[arXiv:1604.06065](#)] [[INSPIRE](#)].
- [2] L. Reverberi et al., in preparation (2019).
- [3] R. Teyssier, *Cosmological hydrodynamics with adaptive mesh refinement: a new high resolution code called ramses*, *Astron. Astrophys.* **385** (2002) 337 [[astro-ph/0111367](#)] [[INSPIRE](#)].
- [4] V. Springel, *The Cosmological simulation code GADGET-2*, *Mon. Not. Roy. Astron. Soc.* **364** (2005) 1105 [[astro-ph/0505010](#)] [[INSPIRE](#)].
- [5] D. Potter, J. Stadel and R. Teyssier, *PKDGRAV3: Beyond Trillion Particle Cosmological Simulations for the Next Era of Galaxy Surveys*, [arXiv:1609.08621](#) [[INSPIRE](#)].
- [6] N.E. Chisari and M. Zaldarriaga, *Connection between Newtonian simulations and general relativity*, *Phys. Rev. D* **83** (2011) 123505 [*Erratum ibid.* **D 84** (2011) 089901] [[arXiv:1101.3555](#)] [[INSPIRE](#)].
- [7] S.R. Green and R.M. Wald, *Newtonian and Relativistic Cosmologies*, *Phys. Rev. D* **85** (2012) 063512 [[arXiv:1111.2997](#)] [[INSPIRE](#)].
- [8] C. Fidler, C. Rampf, T. Tram, R. Crittenden, K. Koyama and D. Wands, *General relativistic corrections to N-body simulations and the Zel'dovich approximation*, *Phys. Rev. D* **92** (2015) 123517 [[arXiv:1505.04756](#)] [[INSPIRE](#)].

- [9] C. Fidler, T. Tram, C. Rampf, R. Crittenden, K. Koyama and D. Wands, *Relativistic Interpretation of Newtonian Simulations for Cosmic Structure Formation*, *JCAP* **09** (2016) 031 [[arXiv:1606.05588](#)] [[INSPIRE](#)].
- [10] M. Borzyszkowski, D. Bertacca and C. Porciani, *LIGER: mock relativistic light-cones from Newtonian simulations*, *Mon. Not. Roy. Astron. Soc.* **471** (2017) 3899 [[arXiv:1703.03407](#)] [[INSPIRE](#)].
- [11] C. Fidler, T. Tram, C. Rampf, R. Crittenden, K. Koyama and D. Wands, *General relativistic weak-field limit and Newtonian N-body simulations*, *JCAP* **12** (2017) 022 [[arXiv:1708.07769](#)] [[INSPIRE](#)].
- [12] S.R. Green and R.M. Wald, *A new framework for analyzing the effects of small scale inhomogeneities in cosmology*, *Phys. Rev. D* **83** (2011) 084020 [[arXiv:1011.4920](#)] [[INSPIRE](#)].
- [13] C. Fidler, T. Tram, C. Rampf, R. Crittenden, K. Koyama and D. Wands, *Relativistic initial conditions for N-body simulations*, *JCAP* **06** (2017) 043 [[arXiv:1702.03221](#)] [[INSPIRE](#)].
- [14] J. Adamek, J. Brandbyge, C. Fidler, S. Hannestad, C. Rampf and T. Tram, *The effect of early radiation in N-body simulations of cosmic structure formation*, *Mon. Not. Roy. Astron. Soc.* **470** (2017) 303 [[arXiv:1703.08585](#)] [[INSPIRE](#)].
- [15] J. Brandbyge, C. Rampf, T. Tram, F. Leclercq, C. Fidler and S. Hannestad, *Cosmological N-body simulations including radiation perturbations*, *Mon. Not. Roy. Astron. Soc.* **466** (2017) L68 [[arXiv:1610.04236](#)] [[INSPIRE](#)].
- [16] C. Fidler, A. Kleinjohann, T. Tram, C. Rampf and K. Koyama, *A new approach to cosmological structure formation with massive neutrinos*, *JCAP* **01** (2019) 025 [[arXiv:1807.03701](#)] [[INSPIRE](#)].
- [17] H. Oyaizu, *Non-linear evolution of $f(R)$ cosmologies I: methodology*, *Phys. Rev. D* **78** (2008) 123523 [[arXiv:0807.2449](#)] [[INSPIRE](#)].
- [18] H. Oyaizu, M. Lima and W. Hu, *Nonlinear evolution of $f(R)$ cosmologies. 2. Power spectrum*, *Phys. Rev. D* **78** (2008) 123524 [[arXiv:0807.2462](#)] [[INSPIRE](#)].
- [19] F. Schmidt, M.V. Lima, H. Oyaizu and W. Hu, *Non-linear Evolution of $f(R)$ Cosmologies III: Halo Statistics*, *Phys. Rev. D* **79** (2009) 083518 [[arXiv:0812.0545](#)] [[INSPIRE](#)].
- [20] B. Li, G.-B. Zhao, R. Teyssier and K. Koyama, *ECOSMOG: An Efficient Code for Simulating Modified Gravity*, *JCAP* **01** (2012) 051 [[arXiv:1110.1379](#)] [[INSPIRE](#)].
- [21] B. Li, W.A. Hellwing, K. Koyama, G.-B. Zhao, E. Jennings and C.M. Baugh, *The nonlinear matter and velocity power spectra in $f(R)$ gravity*, *Mon. Not. Roy. Astron. Soc.* **428** (2013) 743 [[arXiv:1206.4317](#)] [[INSPIRE](#)].
- [22] E. Puchwein, M. Baldi and V. Springel, *Modified Gravity-GADGET: A new code for cosmological hydrodynamical simulations of modified gravity models*, *Mon. Not. Roy. Astron. Soc.* **436** (2013) 348 [[arXiv:1305.2418](#)] [[INSPIRE](#)].
- [23] P. Brax, A.-C. Davis, B. Li, H.A. Winther and G.-B. Zhao, *Systematic Simulations of Modified Gravity: Symmetron and Dilaton Models*, *JCAP* **10** (2012) 002 [[arXiv:1206.3568](#)] [[INSPIRE](#)].
- [24] P. Brax, A.-C. Davis, B. Li, H.A. Winther and G.-B. Zhao, *Systematic simulations of modified gravity: chameleon models*, *JCAP* **04** (2013) 029 [[arXiv:1303.0007](#)] [[INSPIRE](#)].
- [25] C. Llinares, D.F. Mota and H.A. Winther, *ISIS: a new N-body cosmological code with scalar fields based on RAMSES. Code presentation and application to the shapes of clusters*, *Astron. Astrophys.* **562** (2014) A78 [[arXiv:1307.6748](#)] [[INSPIRE](#)].
- [26] J. Adamek, D. Daverio, R. Durrer and M. Kunz, *General Relativistic N-body simulations in the weak field limit*, *Phys. Rev. D* **88** (2013) 103527 [[arXiv:1308.6524](#)] [[INSPIRE](#)].

- [27] J. Adamek, D. Daverio, R. Durrer and M. Kunz, *General relativity and cosmic structure formation*, *Nature Phys.* **12** (2016) 346 [[arXiv:1509.01699](#)] [[INSPIRE](#)].
- [28] T. Clifton, P.G. Ferreira, A. Padilla and C. Skordis, *Modified Gravity and Cosmology*, *Phys. Rept.* **513** (2012) 1 [[arXiv:1106.2476](#)] [[INSPIRE](#)].
- [29] S. Tsujikawa, *Modified gravity models of dark energy*, *Lect. Notes Phys.* **800** (2010) 99 [[arXiv:1101.0191](#)] [[INSPIRE](#)].
- [30] K. Koyama, *Cosmological Tests of Modified Gravity*, *Rept. Prog. Phys.* **79** (2016) 046902 [[arXiv:1504.04623](#)] [[INSPIRE](#)].
- [31] T.P. Sotiriou and V. Faraoni, *$f(R)$ Theories Of Gravity*, *Rev. Mod. Phys.* **82** (2010) 451 [[arXiv:0805.1726](#)] [[INSPIRE](#)].
- [32] A. De Felice and S. Tsujikawa, *$f(R)$ theories*, *Living Rev. Rel.* **13** (2010) 3 [[arXiv:1002.4928](#)] [[INSPIRE](#)].
- [33] S. Capozziello and M. De Laurentis, *Extended Theories of Gravity*, *Phys. Rept.* **509** (2011) 167 [[arXiv:1108.6266](#)] [[INSPIRE](#)].
- [34] W. Hu and I. Sawicki, *Models of $f(R)$ Cosmic Acceleration that Evade Solar-System Tests*, *Phys. Rev. D* **76** (2007) 064004 [[arXiv:0705.1158](#)] [[INSPIRE](#)].
- [35] W. Hu and I. Sawicki, *A Parameterized Post-Friedmann Framework for Modified Gravity*, *Phys. Rev. D* **76** (2007) 104043 [[arXiv:0708.1190](#)] [[INSPIRE](#)].
- [36] L. Pogosian and A. Silvestri, *The pattern of growth in viable $f(R)$ cosmologies*, *Phys. Rev. D* **77** (2008) 023503 [*Erratum ibid.* **D 81** (2010) 049901] [[arXiv:0709.0296](#)] [[INSPIRE](#)].
- [37] S. Capozziello and S. Tsujikawa, *Solar system and equivalence principle constraints on $f(R)$ gravity by chameleon approach*, *Phys. Rev. D* **77** (2008) 107501 [[arXiv:0712.2268](#)] [[INSPIRE](#)].
- [38] M. Martinelli, A. Melchiorri and L. Amendola, *Cosmological constraints on the Hu-Sawicki modified gravity scenario*, *Phys. Rev. D* **79** (2009) 123516 [[arXiv:0906.2350](#)] [[INSPIRE](#)].
- [39] M. Cataneo et al., *New constraints on $f(R)$ gravity from clusters of galaxies*, *Phys. Rev. D* **92** (2015) 044009 [[arXiv:1412.0133](#)] [[INSPIRE](#)].
- [40] M. Baldi, F. Villaescusa-Navarro, M. Viel, E. Puchwein, V. Springel and L. Moscardini, *Cosmic degeneracies — I. Joint N -body simulations of modified gravity and massive neutrinos*, *Mon. Not. Roy. Astron. Soc.* **440** (2014) 75 [[arXiv:1311.2588](#)] [[INSPIRE](#)].
- [41] A.V. Frolov, *A Singularity Problem with $f(R)$ Dark Energy*, *Phys. Rev. Lett.* **101** (2008) 061103 [[arXiv:0803.2500](#)] [[INSPIRE](#)].
- [42] L. Reverberi, *Curvature singularities from gravitational contraction in $f(R)$ gravity*, *Phys. Rev. D* **87** (2013) 084005 [[arXiv:1212.2870](#)] [[INSPIRE](#)].
- [43] J. Noller, F. von Braun-Bates and P.G. Ferreira, *Relativistic scalar fields and the quasistatic approximation in theories of modified gravity*, *Phys. Rev. D* **89** (2014) 023521 [[arXiv:1310.3266](#)] [[INSPIRE](#)].
- [44] C. Llinares and D.F. Mota, *Cosmological simulations of screened modified gravity out of the static approximation: effects on matter distribution*, *Phys. Rev. D* **89** (2014) 084023 [[arXiv:1312.6016](#)] [[INSPIRE](#)].
- [45] I. Sawicki and E. Bellini, *Limits of quasistatic approximation in modified-gravity cosmologies*, *Phys. Rev. D* **92** (2015) 084061 [[arXiv:1503.06831](#)] [[INSPIRE](#)].
- [46] E. Fehlberg, *Klassische runge-kutta-formeln vierter und niedrigerer ordnung mit schrittweiten-kontrolle und ihre anwendung auf wärmeleitungsprobleme*, *Computing* **6** (1970) 61.

- [47] W.H. Press, S.A. Teukolsky, W.T. Vetterling and B.P. Flannery, *Numerical Recipes 3rd Edition: The Art of Scientific Computing*, 3 ed., Cambridge University Press, New York, NY, U.S.A. (2007).
- [48] PLANCK collaboration, *Planck 2018 results. VI. Cosmological parameters*, [arXiv:1807.06209](#) [[INSPIRE](#)].
- [49] D.B. Thomas, M. Bruni, K. Koyama, B. Li and G.-B. Zhao, *f(R) gravity on non-linear scales: The post-Friedmann expansion and the vector potential*, *JCAP* **07** (2015) 051 [[arXiv:1503.07204](#)] [[INSPIRE](#)].
- [50] L. Pizzuti, I.D. Saltas, S. Casas, L. Amendola and A. Biviano, *Future constraints on the gravitational slip with the mass profiles of galaxy clusters*, *Mon. Not. Roy. Astron. Soc.* **486** (2019) 596 [[arXiv:1901.01961](#)] [[INSPIRE](#)].